Final-state symmetry effects in photoemission of thin Gd overlayers

1989 J. Phys.: Condens. Matter 1 6571

(http://iopscience.iop.org/0953-8984/1/37/006)

J. Phys.: Condens. Matter 1 (1989) 6571–6587. Printed in the UK

Final-state symmetry effects in photoemission of thin Gd overlayers

P A Dowben†, D LaGraffe† and M Onellion‡

† Department of Physics, Syracuse University, Syracuse, NY 13244-1130, USA

‡ Department of Physics, University of Wisconsin, Madison, WI 53706, USA

Received 13 December 1988, in final form 2 March 1989

Abstract. The 4f valence band and shallow core levels of ultrathin Gd overlayers on Cu(100) and on crystalline nickel overlayers on Cu(100) have been investigated using angle-resolved photoemission. We have observed a definite selection of final-state symmetries which, for one-half to four-monolayer-thick Gd films, indicates that the occupied Gd 5d band is predominantly $3z^2 - r^2$ and $j = \frac{3}{2}$ in character. The $5p_{3/2}$ appears to be predominantly z in character for thin Gd overlayers on Cu(100). This occurs as a consequence of final-state interactions between the Gd 5d and 5p eigenstates. These results, together with the observed screening processes of the photoemission hole state, are discussed and applied to the understanding of photoemission resonance from the valence bands.

1. Introduction

The investigation of the electronic and magnetic properties of ultrathin (1–10 monolayers) metallic films is an area of increasing interest [1, 2]. The classic problems of magnetism that pertain to the influence of the nearest neighbours, the nearest-neighbour spacings (i.e. homogeneous strain energy [3]), the density of states near the Fermi level and problems associated with reduced dimensionality [1–3], also require some understanding of the electronic (band) structure of the material. Gadolinium is of particular interest because this elemental ferromagnet has been thought to be a classical, localised ferromagnet [4], and unlike the other elemental ferromagnets, Gd is a large-Z element with a number of shallow core levels. Essential to the characterisation of the electronic (band) structure of Gd are the identification of the final-state and initial-state symmetries and an understanding of the many-electron excitations that accompany the photoemission process. The purpose of this investigation was to characterise the final-state symmetries of states that contribute to the valence-band structure of gadolinium thin films, as observed by photoemission.

Cu(100) was chosen as a substrate for the Gd thin-film studies because of the excellent lattice match between the basal plane of HCP Gd (3.64 Å) and FCC copper (3.62 Å) as well as the excellent match between FCC Cu and FCC Ni, providing a comparison between the influence of paramagnetic and ferromagnetic substrates. Furthermore, Cu(100) has proven to be a suitable template for investigating the electronic structure of other high-Z metal overlayers such as Sm [5, 6], Hg [3, 7], Pb [8–10] and Au [11].

2. Experimental procedure

The experiments were performed in an ultra-high-vacuum (UHV) system equipped with a hemispherical analyser with an angular acceptance window of $\pm 1.5°$ for angle-resolved

0953-8984/89/376571 + 17 $02.50

photoemission, as well as a retarding-field analyser for low-energy electron diffraction (LEED). The vacuum system was pumped by a combination of turbomolecular, ion and titanium sublimation pumps, and was equipped with a residual gas analyser and the usual pressure gauges. The hemispherical analyser (50 mm radius) was mounted in the UHV system on a goniometer stage with two degrees of freedom so that a broad range of emission angles in both even and odd geometries (with respect to the mirror plane defined by the vector potential) could be studied.

The light source for the photoemission studies was the 1 GeV ring at the Synchrotron Radiation Centre, dispersed by a 3 m toroidal grating monochromator. The energy resolution of the photoemission spectra collected by the hemispherical analyser varied from 0.15 to 0.4 eV full-width-at-half-maximum (FWHM), including the resolution of the photon source. The operating mode of the hemispherical analyser used for photoemission yielded constant resolution (15 eV pass energy), not constant transmission.

Relative photoemission intensities (constant initial state) [12, 13] were estimated using the maximum intensity of the photoemission feature with the resolution degraded and the intensity normalised with respect to the photon flux from the monochromator, as determined by the yield of a nickel-mesh diode. The electric vector potential $\boldsymbol{A}$ of the incident light was oriented so that the component parallel to the surface was along the Cu $\langle 1\underline{1}0 \rangle$ direction throughout this work (the $\bar{\Gamma}$–$\bar{X}$ direction of the clean Cu(100) surface Brillouin zone). The incidence angle of the light is defined with respect to the surface normal so that normal incidence (zero degrees) has the vector potential completely parallel to the surface (s-polarised) while glancing incidence light has a large component of the vector potential normal to the surface (p-polarised). Photoelectrons were collected normal to the surface throughout this work, except for studies of band dispersion and for angle-resolved Auger studies.

The Cu(100) surface was cleaned by 2 keV Ar^+ ion bombardment and carefully annealed so that a sharp 1×1 LEED pattern was observed. The Cu(100) crystal was cooled to 180–200 K (determined using a nickel–alumel thermocouple), following cleaning and annealing of the Cu(100) crystal. This was done to inhibit the interdiffusion of copper atoms from the Cu(100) substrate into the gadolinium overlayer. Such interdiffusion of copper has been observed with other rare-earth [14] and transition-metal overlayers [1, 11, 15, 16].

The deposition of gadolinium (and nickel) on the Cu(100) substrate was undertaken from metal evaporators after considerable outgassing of the sources. During the evaporation, the base pressure in the system typically rose to pressures between 2×10^{-10} and 5×10^{-10} Torr. Evaporations at higher system pressures were deemed to be unsuitable for study. We found it essential to cool every part of the deposition cell and enclosing shroud, except the actual tungsten filaments containing the metal source, to obtain clean and reproducible deposition. This deposition procedure was found to result in the formation of clean gadolinium thin films determined by Auger electron spectroscopy to have little or no oxygen and carbon contamination. Photoemission studies of the gadolinium films showed little indication of oxygen or carbon contamination (even at photon energies of 20 eV) as can be seen from a comparison of our spectra (figure 1) with photoemission spectra from other gadolinium studies [17, 18].

The thickness of our films was determined using an oscillating-crystal thin-film thickness monitor, but the absolute thickness of our films was also based upon changes in the core-level binding energy shift and the relative gadolinium and substrate photoemission and Auger electron spectroscopy signals. We have used the substrate copper binding energy shifts to establish and confirm gadolinium coverages for coverages up to

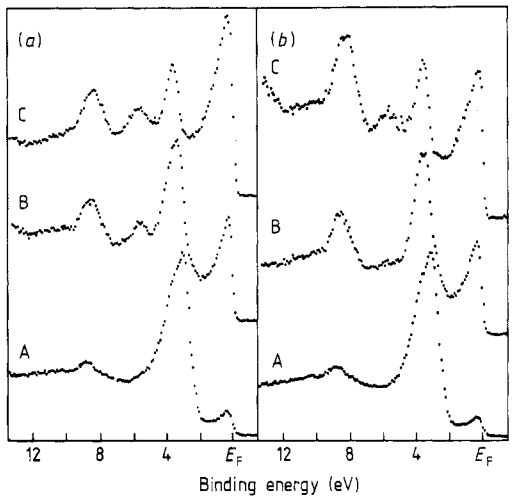

Figure 1. Photoemission spectra for the valence states for Gd overlayers on Cu(100). Spectra are shown for two different light incidence angles of (*a*) 60° and (*b*) 34°, where the electric vector potential is more parallel to the surface normal and the surface respectively. The photoelectrons were all collected normal to the surface and the incident photon energy was 33 eV. All Gd depositions were undertaken at a substrate temperature of 220 K or less. The Gd overlayers are nominally one-half (A), one (B) and two monolayers (C) thick as indicated.

a monolayer (based upon surface to core-level binding energy shift arguments [19–22]). This has allowed us to establish an absolute coverage scale by means which are independent of the thin-film monitor.

As has been shown for other metal overlayers on metal substrates [19], the substrate metal core levels will undergo a binding energy shift with increasing overlayer coverages. The substrate core-level shift is a consequence of a surface to bulk core-level shift. With increasing metal overlayer coverage, the substrate 'surface' core-level signal is suppressed, so that by one monolayer of the overlayer, the surface core-level signal is completely suppressed [19, 28]. By monitoring the Cu core- and valence-level binding energies, completion of one Gd monolayer coverage can be accurately identified. Our relative thickness measurements are accurate to 20%.

To study Gd films on nickel, four monolayers of nickel were deposited onto a Cu(100) sample at room temperature. The overlayers exhibited well ordered 1 × 1 LEED patterns. This Ni/Cu(100) system was cooled to about 150 K before depositing Gd.

3. Results

The photoemission spectra of thin (0–6 monolayer thick films) of gadolinium deposited on Cu(100) asnd on nickel films on Cu(100) are indicative of a density of states in many respects qualitatively similar to that of bulk Gd [4, 23, 24]. The photoemission intensity near the Fermi energy (as seen in figure 1) is largely a result of the Gd 5d bands [4, 23, 24], while the intensity near 8.6 eV binding energy is attributable to the Gd 4f levles [4, 23–27]. The Gd $5p_{1/2}$ and $5p_{3/2}$ shallow core levels may be identified at 26.1 ± 0.4 and 21.9 ± 0.2 eV binding energy respectively (figure 2), consistent with other studies [18]. The photoemission intensity at 3–4 eV below the Fermi energy is due to the Cu(100) d band. The feature at 5 eV is an intrinsic peak, not due to contamination as discussed in more detail elsewhere [28].

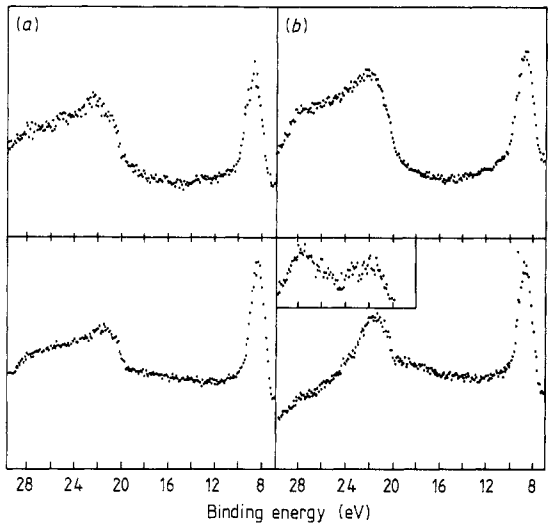

Figure 2. Photoemission spectra of the shallow gadolinium core levels for Gd overlayers on Cu(100). Spectra are shown for two different light incidence angles of (*a*) 34° and (*b*) 60°. The photoelectrons were all collected normal to the surface and the photon energy was 50 eV. The gadolinium overlayers are nominally five and two monolayers thick for the spectra at the top and bottom respectively. Inset: the effect of contamination upon the final-state symmetries of the 5p gadolinium levels at a 60° light incidence angle (note the $5p_{1/2}$ intensity increases or remains unchanged from the spectra at 34° light incidence angle as opposed to the substantial change observed with the clean overlayer).

We note the binding energies of the copper substrate and gadolinium overlayer are dependent upon the gadolinium overlayer thickness. At normal emission the sharp Cu 3d band is at about 3.0 eV below the Fermi energy for clean copper. This binding energy increased to 3.1 eV for a Gd overlayer of nominally half a monolayer and to 3.7 eV for an overlayer nominally one monolayer thick (figure 1). The gadolinium 4f level has a binding energy of 8.8 ± 0.1 eV for thin (½ monolayer) Gd overlayers, and this decreases to 8.6 ± 0.1 eV for one-monolayer films, until for the very thickest films the binding energy is about 8.4 ± 0.1 eV (six monolayers). These core-level shifts are a consequence of surface to bulk core-level shifts and thermodynamically favourable interactions and hybridisation between the gadolinium overlayer and the substrate as discussed in detail elsewhere [28].

It can be seen in figure 1 that the Gd 5d intensity increases with increasing light incidence angles and increasing normal component of the electric vector potential (p-polarised light) with respect to both the Gd 4f levels and the Cu(100) substrate d bands. This effect is more dominant with the thinner (1–2 monolayers) Gd overlayers. Less discernible change in the relative photoemission intensities, with varying light incidence angles, is observed with the thicker Gd overlayers where the Cu(100) photoemission intensities are barely noticeable.

Similarly, for Gd overlayers on Cu(100), in the Gd 5p levels, seen in figure 2, the $5p_{3/2}$ feature is seen to increase relative to both the Gd $5p_{1/2}$ and the Gd 4f levels with increasing light incidence angle for the thinner film, but for the thicker film the relative intensities vary little with light incidence angle. Following background subtraction, the integral intensities of the Gd 5p levels have been used to calculate the $5p_{3/2}$ to $5p_{1/2}$ branching ratios. For the thinner film the branching ratio was found to be 3.38 at 60° incidence angle and 1.7 at a light incidence angle of 32° for a photon energy of 50 eV.

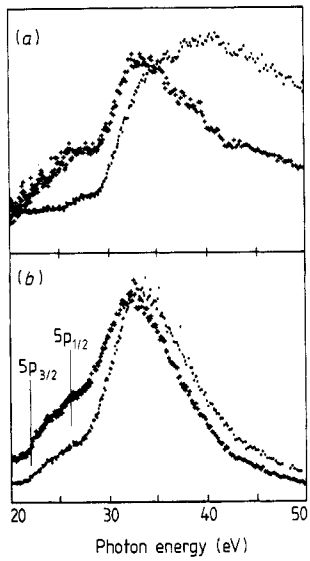

Figure 3. Constant initial-state spectra of the gadolinium (*a*) 4f and (*b*) 5d derived bands. The spectra are for 34° (+) and 70° (●) light incidence angles. All photoelectrons were collected normal to the surface. The nominal thickness of the gadolinium overlayer is one monolayer. The spectra are normalised for the incident photon flux. The $5p_{1/2}$ and $5p_{3/2}$ thresholds are indicated.

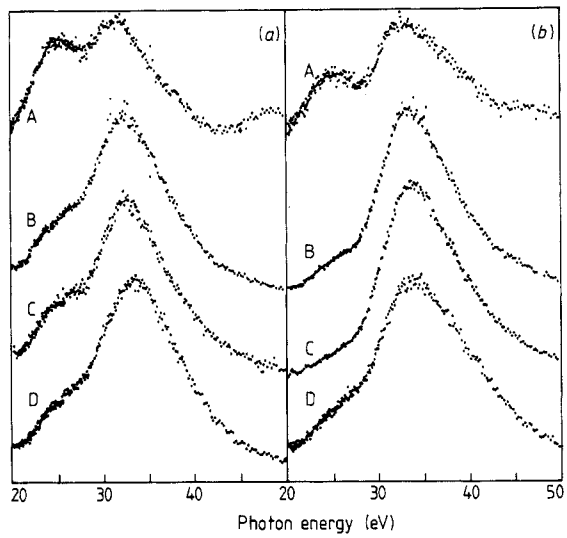

Figure 4. A comparison of the partial cross sections of the gadolinium 5d band for (*a*) 34° and (*b*) 60° light incidence angles. Spectra (constant initial state) are shown for several different thicknesses: A, one-half monolayer; B, one monolayer; C, two monolayers; D, four monolayers.

For the thicker Gd film and the same (50 eV) photon energy, the branching ratios were found to be 2.29 at 32° incidence and 1.91 at 60° incidence.

In order to investigate the variation of the Gd 5d and 4f levels as a function of the incident photon energy, we took constant-initial-state (CIS) spectra for varying gadolinium overlayer thicknesses and light incidence angles as seen in figures 3 and 4. Figure 3 shows that there is a considerable change in the CIS curves as the incidence angle changes. The Gd 5d and 4f partial cross sections, determined from the CIS spectra, both show two pronounced intensity resonances at 25 ± 1 eV and 32 ± 1 eV photon energies. The ratio of the intensity for the two resonance changes for one resonance relative to

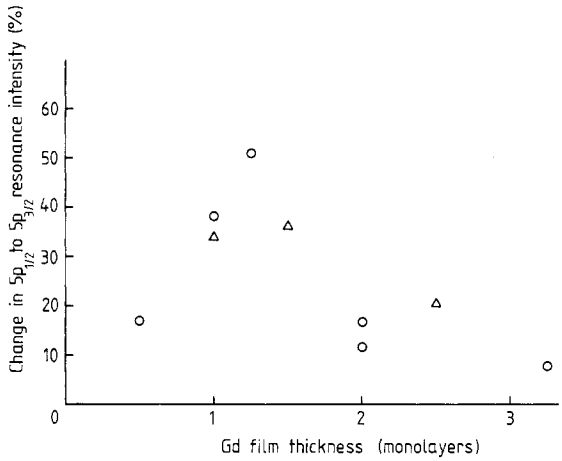

Figure 5. A comparison of the partial cross-section resonances at 25 and 35 Ev for the 5d levels. The relative intensity variation for the two 5d gadolinium resonances at 60° light incidence angle is compared with the ratio at 34° light incidence angle. The difference between the resonant intensity ratio at the two light incidence angles is plotted as a function of coverage (zero change indicates no dependence on light incidence angle). △, Gd/Ni; ○, Gd/Cu.

the other with changing incidence angle (the resonance at 32 ± 1 eV photon energy increases with increasing light incidence angle for both the 4f and the 5d CIS curves). The effect of the light incidence angle upon the Gd 5d partial cross sections is generally more pronounced for thinner gadolinium films as seen in figures 4 and 5, although for the very thinnest of films investigated, the relative change in the 25 and 32 eV photon energy resonances with changing light incidence angle is reduced as demonstrated in figure 5.

The photoemission intensity resonances are clearly broader (greater FWHM) at light incidence angles nearer to grazing (70°) incidence. For the 4f CIS spectra, additional photoemission intensity can be observed with photon energies above 35 eV p-polarised light (with large light incidence angles) while this photoemission intensity is not observed with s-polarised light (more normal incidence angles).

The position of the additional density of states near the Fermi level following the deposition of small amounts of gadolinium is affected by the substrate, as can be seen in figure 6. For Gd overlayers on nickel (deposited on the Cu (100) substrate), the maximum d-band intensity is 1.5–1.6 eV from the Fermi energy, while for Gd overlayers deposited on the clean Cu(100) substrate, the d-band density of states is at the Fermi energy.

Angle-resolved Auger electron spectroscopy and LEED studies of the growth mode are strongly indicative of a 'simultaneous multilayer' [29] overlayer growth mode that only resembles layer-by-layer growth for the first monolayer [30]. As seen in figure 7, thin films of gadolinium on Cu(100) show an emission-angle dependence of the Gd 895 eV Auger electron signal against the Cu 920 eV Auger electron signal that increases with increasing emission angle. Ideally with no interdiffusion, the Gd-to-Cu signal intensity should obey the relationship $I(x) = a + b/\cos(x)$ [31]. Using a least-squares fit to the data obtained at 20 and 60 °C, a theoretical curve based upon expected results without interdiffusion has been generated for comparison with the data. From a compilation of such studies it is apparent that Gd interdiffusion with the Cu is substantial at temperatures near 100 °C (see figure 7), but for similar depositions at lower temperatures the gadolinium films are fairly uniform and diffusion is suppressed.

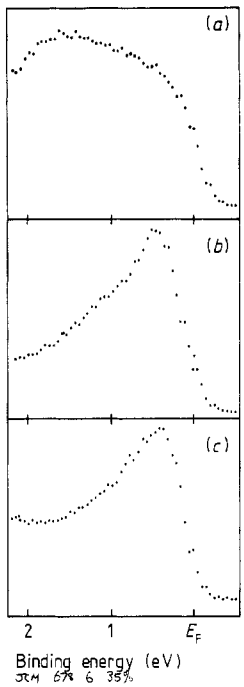

Figure 6. Energy distribution curves showing the density of states near the Fermi energy for two-monolayer thick Gd overlayers on (*a*) nickel and (*c*) copper. For all of the photoemisson spectra the photon energy is 33 eV, and the light incidence angle is 60° with respect to the surface normal to favour selection of $3z^2 - r^2$ character bonds. All photoelectrons were collected normal to the surface. The Ni 3d band for Ni on Cu(100) is shown in (*b*) and is clearly quite different from that in (*a*).

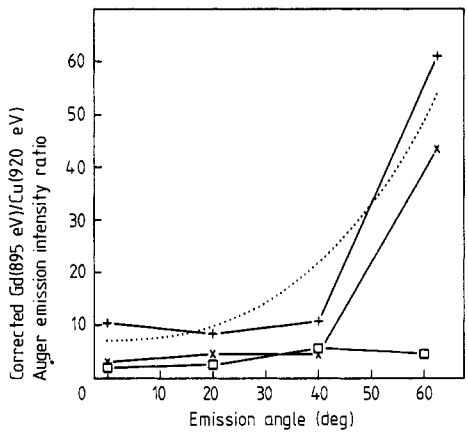

Figure 7. The emission angle dependence of the gadolinium 895 eV Auger electron signal with respect to the Cu 920 eV Auger electron signal. The results are plotted for several different annealing temperatures as indicated: +, 20 °C; ×, 60 °C; □, 100 °C. The results for 20 and 60 °C are compared with a $1/\cos\theta$ dependence by a least-squares fit. The dotted curves is that given by theory.

For the gadolinium overlayers no evidence of long-range order in low-energy electron diffraction was observed. Very diffuse diffraction beams suggestive of a c(2 × 2) overlayer were observed with very thin gadolinium overlayers. Our meagre structural information is consistent with a random-site adsorption model [30] where little diffusion of the overlayer gadolinium is present. For c(2 × 2) overlayers, statistical calculations based upon adsorption without diffusion [30] have indicated that a significant fraction of the first monolayer is completed (approximately 80–90%) before there is a significant LEED contribution from the second layer.

4. Discussion

With angle-resolved photoemission from overlayers, there are a number of light polarisation and symmetry effects that can be observed [1, 32–35]. In particular, the symmetry

and selection rules for direct interband transitions, in the one-electron picture, are derived from Fermi's golden rule expression:

$$\sigma(\omega) = 4\pi^2 \alpha \hbar\omega \sum_{f,i} |\langle f|E \cdot U_{ext}(x)|i\rangle|^2 \delta(\hbar\omega - E_F + E_i)$$

where f is the final-state eigen-function, i is the initial-state eigenfunction, and $E \cdot U_{ext}(x)$ is the interaction potential proportional to $A \cdot p$ [1, 33, 34, 36]. As a result, the symmetry of the initial state must be the same as that of the perturbed Hamiltonian operator and the final state in order to have a non-zero matrix element. With photoemission, the symmetry of the final state can be determined to some extent. Even though there is no evidence of long-range order for the gadolinium overlayers, the final-state symmetry of the eigen-states can be probed by altering the orientation of the electric vector potential with respect to the surface normal. The lack of crystalline order does relax the symmetry selection rules somewhat [1, 32–34], as does the need for relativistic dipole selection rules [35]. It is, of course, essential to collect the photoelectrons normal to the surface, particularly for the disordered overlayer, to obtain information upon the final-state symemtries.

We can divide our discussion of the final-state symmetry effects into those for the 5d, 5p and 4f levels. We have undertaken this analysis in order to demonstrate a final-state interaction of the Gd 5d conduction band and shallow (in our case 5p) core levels. It is important to understand that a number of many-electron processes are part of photoemission from rare-earth overlayers. From the golden rule expression, we can often infer the symmetry of the initial state, essential for the characterisation of the electronic (band) structure. This analysis has largely been applied to Gd overlayers on Cu(100) (unless noted otherwise) and some comparison is made with Gd overlayers on Ni. The absorption of Gd at 150–200 K does put the gadolinium overlayer at a temperature well below the critical temperature for ferromagnetism for bulk Gd [37–39]. Nonetheless, mapping out the band structure to compare with calculations for the bulk may be a fruitless exercise in view of the absence of long-range order and the absence of any observed dispersion under our deposition conditions. Our results are not to be taken as representative of bulk gadolinium.

4.1. The character of the Gd 5d band

As a consequence of the above selection rules, eigen-states with s, p_z and $d_{z^2-r^2}$ character are preferentially selected over other p and d states in angle-resolved photoemission when the electric vector potential of the incident light is oriented normal to the surface (p-polarised light) and cannot generally be observed when the vector potential is in the plane of the surface. With increasing incidence angle, and when a greater component of the vector potential is oriented normal to the surface, the intensity of the gadolinium 5d band increases with respect to the Cu 3d bands and the more atomic-like (hence more isotropic) Gd 4f levels with normal emission. We therefore conclude that the initial-state symmetry of the occupied Gd 5d band is of $3z^2 - r^2$ character, from the dependence on angle of incidence demonstrated in figure 1.

Conduction-band states of a particular initial-state symmetry will interact with the substrate according to the symmetry and disposition of the substrate bands. The Gd 5d bands (of $3z^2 - r^2$ character) are clearly influence by the substrate. The hybridisation of the Gd 5d band with the Ni 3d band would result in an increase of the Gd 5d-band binding energy, particularly since the Ni 3d band has appreciable $3z^2 - r^2$ character well below E_F [40, 41] (a bonding-like configuration). The greater Gd 5d binding energy on

nickel than copper, as observed in figure 6, is consistent with changing hybridisation of the Gd 5d bands with the substrate. This hybridisation of the gadolinium overlayer with the substrate occurs principally with the 5d levels and not the 4f levels, since for similar gadolinium overlayer thicknesses the 4f binding energy is approximately the same on both nickel and copper. This hybridisation is consistent with the character assignment of the Gd 5d band. The strong hybridisation of the gadolinium overlayer with the nickel substrate does, in part, support the suggestion of antiferromagnetic coupling of gadolinium overlayers with iron [42].

Further indications supporting our assignment of a $3z^2 - r^2$ initial-state character to the Gd 5d state may be found from an examination of the partial photoemisison cross sections of the Gd 5d state. We note that the FWHM of the photoemission resonances (whose origin and character will be discussed in detail below) is greater when the $3z^2 - r^2$ character of the Gd 5d band is preferentially selected, as seen in figures 3 and 4. The increase in the photon energy range, for which the partial cross section of the 5d band is substantial, tends to suggest an increase in the screening of the initial state [43, 44] of $3z^2 - r^2$ symmetry. Such screening of the initial state can be a consequence of the hybridisation of eigen-states from adjacent adatoms to form a band [44, 45]. We conclude above that for gadolinium overlayers on Cu(100) at 200 K, adjacent adatoms hybridise to form a band and that band is predominantly of $3z^2 - r^2$ character. Such a band is also far more likely to mix with a band formed from the gadolinium 6s electrons since both share the same symmetry on a C_{4v} surface (as would be the symmetry of a c(2 × 2) overlayer on Cu(100)).

The dependence on light incidence angle of the 5d photoemission feature is more pronounced for one- to two-monolayer Gd films than for six-monolayer films on Cu(100). We believe that the film thickness affects the apparent initial-state symmetry of the Gd 5d level and may be a consequence of increasing numbers of defects in the film. We suggest that the Gd overlayer growth mode is akin to simultaneous multilayer growth [29] and the large defect density with island growth for the thicker Gd films may obscure symmetry and polarisation selection resulting from even local (short-range) order [30]. For half-monolayer films, the Gd overlayer is not complete, and islands of Gd, not covering the Cu(100) substrate, also act to reduce the symmetry anisotropy of the occupied Gd 5d bands. Annealing the Gd overlayer, while possibly increasing long-range order and improving the observed light polarisation effects in photoemission, is almost certain to result in interdiffusion of the Cu from the substrate with the overlayer, resulting in an overlayer far more difficult to characterise [11, 14–16], as indicated by figure 7.

4.2. The Gd 5d photoemission resonances

Resonant enhancement of the valence-band photoemission features has been observed for a number of metals (references [18, 36, 43, 46] and references therein) as well as for gadolinium overlayers [18]. The resonant enhancement of the Gd 5d band, as well as for other rare earths, has been successfully explained in terms of a 5p excitation of a low-lying *nl* excited electron state (mainly of 5d character) which decays via a super Coster–Kronig transition:

$$5p^6 4f^7 5d^1 6s^2 \rightarrow 5p^5 4f^7 5d^2 6s^2 \rightarrow 5p^6 4f^7 5d^0 6s^2 + e^-$$

resulting in a final state identical to the direct 5d emission [18, 36]. The two excitation pathways can resonate, often resulting in an interference dip characteristic of a Fano

resonance. In addition, Auger decay to final states such as $5p^6 4f^7 5d^1 6s^1$ and $5p^6 4f^7 5d^2 6s^0$ may also occur to some extent. Auger decay to the $5p^6 4f^6 5d^1 6s^2$ and $5p^6 4f^6 5d^2 6s^1$ contributes only to the 4f levels (at selected photon energies of course) and does not contribute to the 5d photoemission resonances.

The photoemission resonances observed (as seen in figures 3 and 4) for the Gd 5d band at the photon energies of 25 and 32 eV are a result of this 5p–5d interaction and occur just above the $5p_{3/2}$ and $5p_{1/2}$ thresholds at 21.9 ± 0.2 eV and 26.1 ± 0.4 eV respectively [18]. Since the resonance at the $5p_{1/2}$ threshold is consistently more intense than that at the $5p_{3/2}$ threshold, despite the greater theoretical electron occupancy of the $5p_{3/2}$ state, the dipole selection rules dictate that the low-lying *nl* excited electron state is mainly of $5d_{3/2}$ character since, for a photoexcitation, dipole selection dictates that $\Delta l = \pm 1$, $\Delta j = 0, \pm 1$.

A $d_{5/2}$ unoccupied state at the Fermi energy would not be consistent with this observation. The large-Z nature of gadolinium as well as extra-atomic excitations (expected as a consequence of the hybridisation of 5d eigen-states to form bands [43, 44]) is expected to result in the relaxation of the dipole selection rules, permitting a number of generally forbidden excitations to occur. The presence of pronounced spin–orbit interactions of the 5p levels necessitates the use of relativistic dipole selection rules [35] which differ somewhat from the non-relativistic one-electron dipole selection rules. These effects which relax the dipole selection rules do not, however, alter the above interpretation assigning the unoccupied d band at the Fermi energy $j = \frac{3}{2}$ character. Hund's rule suggests that, since the unoccupied band at the Fermi energy is of $j = \frac{3}{2}$ character, the occupied d band is also of the same character. Indeed, this character assignment is generally consistent with Hund's rule concerning the occupancy of levels.

Careful analysis of the results presented in figures 3 and 4 indicates that, for s-polarised light, the $5p_{1/2}$ to 5d photoemission resonance for gadolinium on Cu(100) peaks at 31.5 eV photon energy for one-, two- and three-monolayer thick films. For p-polarised light, this photoemission resonance is at a maximum at 32.6 eV for one monolayer, 32.4 eV for two monolayers and 32.3 eV for three monolayers. Application of Fermi's golden rule suggests that, since the $5p_{1/2}$ initial-state symmetry selected in the photoemission process is altered with the changing light polarisation, the symmetry of the empty 5d gadolinium state involved in the resonant photoemission process is also altered. We therefore conclude that the unoccupied $d_{xz,yz}$ character states are closer to the Fermi level than the unoccupied $d_{3z^2-r^2}$ character states by 1.1 eV for films one monolayer thick, 0.9 eV for films two monolayers thick and 0.7 eV for films three monolayers thick (using monolayer equivalents) of gadolinium on Cu(100). Our results for thicker gadolinium overlayers on Cu(100) are consistent with similiar studies for thick gadolinium films using circularly polarised light [47].

4.3. The character of the 5p gadolinium levels

Both the energy distribution curves (figure 2) as well as the CIS spectra of the gadolinium 5d band across the 5p thresholds (figures 3, 4 and 5) are affected by changes in light incidence angle. Since these photoemission studies probe excitations from the 5p levels, we can infer the final-state symmetry of the 5p levels for Gd overlayers on Cu(100). The increasing photoemission (figure 2) intensity of the gadolinium $5p_{3/2}$ level (with respect to the nominal $5p_{1/2}$ feature and the 4f level) with increasing incidence angle suggest that, as with the Gd 5d band appearing to be of $3z^2 - r^2$ character, the $5p_{3/2}$ state has sizable p_z character. The relative loss in intensity of the $5p_{1/2}$ state with increasing

Table 1. 5p eigen-state spinors, characters and spins.

j	m_j	Spinor	Character	Spin
$\frac{3}{2}$	$\frac{3}{2}$	y	no p_z	Spin-up
	$-\frac{3}{2}$	1	no p_z	Spin-down
	$\frac{1}{2}$	$\frac{1}{\sqrt{3}}\begin{pmatrix}\sqrt{2}\,y_1^0\\ y_1^1\end{pmatrix}$	$\frac{2}{3}p_z$	—
	$-\frac{1}{2}$	$\frac{1}{\sqrt{3}}\begin{pmatrix}y_1^{-1}\\ \sqrt{2}\,y_1^0\end{pmatrix}$	$\frac{2}{3}p_z$	—
$\frac{1}{2}$	$\frac{1}{2}$	$\frac{1}{\sqrt{3}}\begin{pmatrix}-y_1^0\\ \sqrt{2}\,y_1^1\end{pmatrix}$	$\frac{1}{3}p_z$	—
	$-\frac{1}{2}$	$\frac{1}{\sqrt{3}}\begin{pmatrix}-\sqrt{2}\,y_1^{-1}\\ y_1^0\end{pmatrix}$	$\frac{1}{3}p_z$	—

$y_1^0 = p_z$, $y_1^1 = p_x + ip_y$, $y_1^{-1} = p_x - ip_y$.

incidence angle (and correspondingly a greater vector potential component normal to the surface) indicates that there is little p_z character in the $5p_{1/2}$ state and, in principle, this level should be therefore largely linear combinations of $p_x \pm ip_y$.

The spatial anisotropy of shallow core levels, this far below the Fermi energy, is particularly difficult to understand in view of the observation (figure 2) that this anisotropy for the 5p levels 21 and 26 eV below the Fermi energy is greater than that for the 4f level at about 8.6 eV binding energy. Shallow core levels can be considered part of the valence band [1, 48], and for gadolinium the 4f level needs to be considered part of the valence band [4]. The 5p levels, nonetheless, should remain relatively spatially isotropic. Our results are not consistent with the 5p initial-state symmetries suggested by the eigen-state spinors listed in table 1.

There are few reasons that can be invoked to explain these unusual results, and the nature of the explanation depends upon whether the character of the p levels is a consequence of the initial state or the photoemission final state. Final-state effects appear to provide the most plausible explanation of the observed polarisation effects observed with the angle-resolved photoemission from gadolinium overlayers.

We have considered the influence of band-structure formation, symmetry and magnetism upon the initial-state symmetries of the Gd 5p state, but cannot reconcile the effects with our observed photoemission results. Symmetry breaking as a result of the reduced dimensionality of the gadolinium overlayer can result in the lifting of the degenerate character of p levels [48], but this requires formation of band structure as well and, for core levels more than 10 eV below E_F, this band-structure formation must be regarded as generally absurd, particularly to the degree necessary to lift the degeneracies necessary to reproduce the above results (a p-level separation of approximately 6 eV). The calculations for bulk gadolinium [23] indicate that the core-level 5s and 5d states from adjacent atoms do overlap to form bands, but the bandwidths are only about 1 eV, which is not sufficient to explain the present data.

The p_x, p_y and p_z orbitals are simply x, y, z times a spherical wavefunction. Without spin–orbit coupling (in which case L_z remains a good quantum number) we can define the eigen-states $Y_1^{-1} = p_x - ip_y$ ($m_l = -1$), $Y_1^0 = p_z$ ($m_l = 0$) and $Y_1^1 = p_x + ip_y$ ($m_l = 1$). In the presence of a magnetic field (recall that gadolinium is nominally ferro-

magnetic with a magnetic moment of approximately $7.7\mu_B$) the p-level degeneracy might be lifted, even if there is a small amount of spin–orbit coupling [49]. Some aspects of our results might be consistent with such a model; however, we observe that the p-level degeneracy is lifted into two features and not three as would be expected from the influence of the magnetic field alone. Furthermore, the separation between the two p-like levels is quite large (6 eV), which is not expected with such a model. The two features cannot be a result of the separation of the p level into the majority and minority bands either, since the exchange splitting would preserve the spatial symmetry of the bands. We should note that the internal magnetic field of the gadolinium cannot be eliminated as having a possible influence in the initial-state electronic structure of the core levels and their resulting spatial symmetry. A strong magnetic field will polarise even a spherically symmetric eigen-state such as an s level resulting in a compression of the state in the z direction (assumed to be the direction of the field) and expanding the wavefunction in the x–y plane. Similarly, a strong field normal to the surface would decrease the binding energy of states with a p_z component with respect to a state like Y_1^{-1} (assuming the correct orientation of the field) since such a state has no dipole moment that can be aligned with the field. Some spin polarisation of the 5p states is expected for bulk gadolinium [23].

With spin–orbit coupling J_z, J^2, L^2 and S^2 are constants of motion and commute with the Hamiltonian (i.e. are good quantum numbers) while L_z and S_z are not good quantum numbers. The eigen-states for the p level with spin–orbit coupling, but in the absence of a magnetic field, must be described by spinors and may be explicitly written with commonly used notation [49] as has been done in table 1. As should be noted, the initial eigen-states suggest that, in the absence of a magnetic field, there is an equal amount ($\frac{1}{3}$) of p_z, $p_x + ip_y$ character in both the $5p_{1/2}$ and $5p_{3/2}$ levels and that the $5p_{3/2}$ levels should not be predominantly p_z in character as is observed. A magnetic field would be expected not to alter this level ordering except to lift the degeneracies in the 5p levels. The initial eigen-states are not therefore consistent with our photoemission results from the gadolinium 5p levels. We must then look to the final state to explain our photoemission results.

Final-state effects must be considered in any photoemission study, particularly of the rare earths, and the most likely explanation for our results is that there are dominant final-state effects in the photoemission and photoexcitation of electrons from shallow core levels. Excitations to the 4f unoccupied levels (approximately 4 eV above the Fermi energy for gadolinium) are very common with the rare earths and can result in shake-up satellites [50]. While such photoemission excitations undoubtedly occur and are partly responsible for the photoemission intensity at 5 eV binding energy [28], we cannot explain our results for the 5p gadolinium states by coupling the 5p levels with the 4f level in the photoemission process. This is partly a consequence of the necessity of reconciling the observed spatial anisotropy of the 5p levels with the spatial isotropy of the 4f levels. Furthermore, final states resulting in an electron in the unoccupied 4f level as a part of a many-electron excitation would result in 'shake-up' satellite structures which are not observed. The observed 5p Gd features (figure 2) cannot be reconciled with shake-up processes because the CIS results from the gadolinium 5d levels (at the Fermi level) exhibit the well defined $5p_{1/2}$ and $5p_{3/2}$ photoemission resonance excitation structures [18] (accompanied, it should be noted, by considerable light incidence angle dependence). Nonetheless, we note that, for the rare earths, core-level photoemission studies can exhibit strong 4f coupling for many core levels [51]. Final-state effects, while perhaps not resulting from significant 4f contributions, can certainly result from 5d coupling contributions.

Because of the symmetry restrictions upon the final state, as indicated above, the ion left after a photoemission event must have a symmetry similar to the orbital from which the photoelectron was ejected. The total symmetry requirement is satisfied by coupling with the wavefunction of the outgoing electron. This symmetry restriction requires that photoemission from the $5p_{3/2}$ level can yield an s-like and a d-like wave, but the symmetry of the resulting ion is $^2P_{3/2}$, assuming no other contributions from other electrons in the atom. This suggests that the outgoing wave is d-like.

These exchange interactions of the valence d states with lower-lying core levels will affect the apparent binding energies of the core electrons. This effect results in the phenomenon known as multiplet splitting which has been studied in great detail for the 4s and 5s subshells in the rare earths [52, 53]. The observed multiplet splitting, which is roughly a measure of the exchange interactions between the unpaired valence electrons with the core electrons (affecting, it should be noted, electrons with spin-up and spin-down character in a substantially different manner), is greatest for gadolinium among all the rare earths [52, 53]. The multiplet splitting of the 5p levels would tend to result in an increased separation of the apparent 'spin–orbit' doublet [54–56]. If only exchange polarisation is considered, however, only two strong 5p features would be observed as a result of the 5d interaction with the 5p hole [54, 55].

Thus final-state effects, resulting from the post-ionisation overlap of the 5d wavefunction (or the 6s) with the 5p corehole are, at least superfically, consistent with our data, particularly in view of the large (approximately 6 eV) separation between the 5p features [54]. Given that this exchange polarisation is strongly dependent upon the spin [55, 57], the fact that the results may be interpreted as indicating that the 5d–5p interaction posibly imparts the 5d symmetry character $(3z^2 - r^2)$ more to the $5p_{3/2}$-like level than the $5p_{1/2}$ level is not surprising. Thus the apparent character of the $5p_{3/2}$ level may be attributable to final-state effects, which must also increase the level separation as well as alter the apparent branching ratios from the statistical value [55]. In the light polarisation selection geometry of our experiments, s and $d_{3z^2-r^2}$ character is virtually indistinguishable from p_z character, by photoemission. We are observing a final-state symmetry of the 5p levels as a consequence of 5d–5p interactions and the $3z^2 - r^2$ initial-state character of the 5d band.

We note that the final-state symmetry selection of the 5p level is substantially altered by contamination (as seen in figure 2), though not the level splitting. With contamination, the $5p_{1/2}$ level also acquires substantial p_z-like character. This favours an explanation of the photoemission results that invokes a final-state effect as proposed above, since the final-state symmetry would be altered as a consequence of impurity hybridisation with the Gd 5d band. An explanation that is based upon initial-state hybridisation of the core 5p levels would, however, have both the symmetry and level splitting altered by impurities.

4.4. The Gd 4f photoemission resonances

We have observed photoemission resonances not only for the Gd 5d band, but also for the Gd 4f level, as demonstrated in figure 3. Similar to the Gd 5d band, there are resonances at the $5p_{1/2}$ and $5p_{3/2}$ thresholds, although the enhancement of the 4f level must occur as a consequence of an Auger-like decay mechanism:

$$5p^6 4f^7 5d^1 6s^2 \rightarrow 5p^5 4f^7 5d^2 6s^2 \rightarrow 5p^6 4f^6 5d^1 6s^2 + e^-$$

but the initial excitation retains many of the properties observed with the Gd 5d band

resonances. Again, the ion final state is the same as occurs with the direct photoemission process.

The additional photoemission intensity contribution to the 4f level observed with large incidence angle at photon energies above 35 eV can also be a consequence of an excitation from the Gd 5s level. The Gd 5s level is, as discussed above, a multiplet split doublet [52, 53] with a binding energy variously ascribed from 35 eV [58] to 43.5 eV [52]. An excitation from the 5s level resulting in a resonance is consistent with this binding energy as is the observation that this additional photoemission intensity to the 4f level occurs principally with large incidence angles. With large light incidence angles a greater component of the electric vector potential is oriented normal to the surface, which is the most favourable orientation for coupling with an s-character eigen-state [1, 32–34].

Excitation from core s-character states have been observed to result in photoemission resonances for 3d transition metals such as nickel [59] and may therefore be expected for gadolinium. An s to d excitation is forbidden by the dipole selection rules but an citation to the sp band is allowed [59]. The nature of this 6p-like state is ill defined for the solid, but may be possibly localised due to the presence of the core hole. The 5s to 6p transition at the 5s threshold,

$$5s^2 5p^6 4f^7 5d^1 6s^2 \rightarrow 5s^1 5p^6 4f^7 5d^1 6s^2 6p^1,$$

can now decay via the direct recombination process and subsequent Auger decay:

$$5s^1 5p^6 4f^7 5d^1 6s^2 6p^1 \rightarrow 5s^2 5p^6 4f^6 5d^1 6s^2 + e^-.$$

These excitation processes will resonate with the direct 4f emission:

$$5s^2 5p^6 4f^7 5d^1 6s^2 \rightarrow 5s^2 5p^6 4f^6 5d^1 6s^2 + e^-.$$

Other Auger decay processes can also take place and contribute to the 4f intensity at selected photon energies, such as

$$5s^1 5p^6 4f^7 5d^1 6s^2 6p^1 \rightarrow 5s^2 5p^6 4f^7 5d^0 6s^1 6p^1 + e^-$$

and

$$\rightarrow 5s^2 5p^6 4f^7 5d^1 6s^0 6p^1 + e^-$$

and

$$\rightarrow 5s^2 5p^6 4f^7 5d^0 6s^2 + e^-$$

as well as the Auger processes described previously in our discussion of the Gd 5d resonances. However, some Auger decay modes will not contribute to the 4f intensity. These include

$$5s^1 5p^6 4f^7 5d^1 6s^2 6p^1 \rightarrow 5s^2 5p^6 4f^6 5d^1 6s^1 6p^1 + e^-$$

and

$$\rightarrow 5s^2 5p^6 4f^6 5d^0 6s^2 6p^1 + e^-.$$

Given the many excitations and decay processes occurring, this will serve to make the 5s to 6p and 5p to 5d (in p-polarisation) contributions to the 4f photoemission resonance very broad, as does the large half-width of the initial 5s state. This is consistent with the featureless photoemission intensity increase to the 4f level above 35 eV photon energy as seen in figure 3. There may be similar processes occurring with the 5d band, but given that the 5d band is at the Fermi energy, many of these Auger decay mechanisms

cannot contribute or can contribute only very weakly to the 5d initial-state intensity. These many-electron excitation and decay processes are numerous and should be considered in any analysis of photoemission results from the rare earths.

At photon energies above 35 eV, the 4f partial cross section is sufficiently different in p-polarisation from in s-polarisation that the photoemission results are consistent with a final-state symmetry similar to that observed for the 5d and $5p_{3/2}$ level. At some photon energies the 4f level appears to be of the same symmetry group as s, p_z and $d_{3z^2-r^2}$. This also indicates that the p_z-like symmetry of the 5p levels is quite pronounced since this spatial anisotropy is referenced to the 4f levels at 50 eV photon energy.

5. Conclusions

Using photoemission to investigate thin gadolinium overlayers on Cu(100) we have been able to determine the final-state symmetry of the $5p_{3/2}$ and 5d levels of gadolinium. Assuming that the gadolinium atoms adsorb into a local c(2 × 2) geometry so that the overlayer preserves, at least locally, the C_{4v} symmetry of the substrate, the $5p_{3/2}$ and 5d eigen-states have Δ_1 symmetry (s, p_z or $d_{z^2-r^2}$) at normal emission, while the $5p_{1/2}$ has Δ_5 symmetry (p_x, p_y, d_{xz} or d_{yz}). These photoemission final-state symmetries are a consequence of final-state 5p–5d interactions. The spin is clearly very important to understanding these many-electron processes, suggesting that some spin polarisation does occur in the photoemission process from gadolinium thin films. Valence-to-core final-state interactions leading to multiplet splittings are a common consequence of photoemission from d-band magnetic materials.

There is evidence that the gadolinium 5d states are $3z^2 - r^2$ and $j = \frac{3}{2}$ in character in the initial state for ultra-thin gadolinium overlayers on copper and nickel. There are also strong indications that the 5d states are hybridised to form a band for one- and two-monolayer thick films. The unoccupied 5d states of $5d_{3z^2-r^2}$ and $5d_{xz,yz}$ character are separated by at least 0.6 eV for thicker films and 1.1 eV for thinner films with the unoccupied $5d_{xz,yz}$ character states lying closer to the Fermi energy.

It is clear that photoemission from gadolinium is complicated by a number of many-electron processes. These many-electron processes make photoemission of rare-earth overlayers particularly complex and substantially alter the photoemission partial cross sections. The many-electron excitations must be characterised if we are to use photoemission to determine the electronic structure of the rare earths.

Acknowledgments

This work was funded by the US Department of Energy through grant DE-FG-02-87-ER-45319. The authors would like to thank C G Olson and A Miller for a number of particularly useful conversations. This work was undertaken at the Synchrotron Radiation Center in Stoughton, Wisconsisn, which is funded by the National Science Foundation.

References

[1] Dowben P A, Onellion M and Kime Y J 1988 *Scanning Microsc.* **2** 177

[2] Erskine J L, Onellion M F and Thompson M A 1987 *Proc. Mater. Res. Soc. Symp.* (Pittsburgh Materials Research Society)

[3] Dowben P A, Varma S, Kime Y J, Muellen D R and Onellion M 1988 *Z. Phys.* B **73** 247
[4] Sticht J and Kubler J 1985 *Solid State Commun.* **53** 529
[5] Faldt A and Myers H P 1985 *J. Magn. Magn. Mater.* **47/48** 225
[6] Faldt A and Myers H P 1984 *Phys. Rev. Lett.* **52** 1315
[7] Onellion M, Kime Y J, Dowben P A and Tache L 1987 *J. Phys. C: Solid State Phys.* **20** L633
[8] Hosler W and Moritz W 1986 *Surf. Sci.* **175** 63
[9] Sepulveda A and Rhead G E 1977 *Surf. Sci.* **66** 436
[10] Henrion J and Rhead G E 1972 *Surf. Sci.* **29** 20
[11] Graham G W 1987 *Surf. Sci.* **184** 134
[12] Lapeyre G J, Baer A D, Hermanson J, Anderson J, Knapp J A and Gobby P L 1974 *Solid State Commun.* **15** 1601
[13] Lapeyre G J, Anderson J, Gobby P L and Knapp J A 1977 *Phys. Rev. Lett.* **33** 1290
[14] Wieliczka D M and Olson C G *Phys. Rev.* B submitted
Olson C G 1988 private communication
[15] Steigerwald D A and Egelhoff W F Jr 1987 *Surf. Sci.* **192** L887
[16] Steigerwald D A, Jacob I and Egelhoff W F Jr 1988 *Surf. Sci.* **202** 472
[17] Wandelt K and Brundle C R 1985 *Surf. Sci.* **157** 162
[18] Murgai V, Huang Y-S, denBoer M L and Horn S 1988 *Solid State Commun.* **66** 329
[19] Egelhoff W F Jr 1987 *Surf. Sci. Rep.* **6** 253
[20] Egelhoff W F Jr 1984 *Phys. Rev.* B **29** 4769
[21] Egelhoff W F Jr 1983 *Phys. Rev. Lett.* **50** 587
[22] Morris W A, Webber P R and Zhang Z G 1988 *Thin Solid Films* **156** 65
[23] Harmon B N and Freeman A J 1974 *Phys. Rev.* B **10** 1979
[24] Dimmock J O and Freeman A J 1964 *Phys. Rev. Lett.* **13** 750
[25] Lang J K, Baer Y and Cox P A 1981 *J. Phys. F: Met. Phys.* **11** 121
[26] Kammerer R, Barth J, Gerken F, Flodstrom A and Johansson L I 1982 *Solid State Commun.* **41** 435
[27] McFeely F R, Kowalczyk S P, Ley L and Shirley D A 1973 *Phys. Lett.* **45A** 227
[28] LaGraffe D, Dowben P A and Onellion M 1989 *Phys. Rev.* B at press
[29] Barthes M G and Rolland A 1981 *Thin Solid Films* **76** 45
[30] Flynn D K, Evans J W and Thiel P A 1989 *J. Vac. Sci. Technol.* A **7** 2162
Evans J W 1989 *Phys. Rev.* B **39** 5655
[31] Fardley C S 1978 *Electron Spectroscopy: Theory, Techniques and Applications* vol 2, ed. C R Brundle and A D Baker (New York: Academic)
[32] Scheffler M, Kambe K and Forstmann F 1978 *Solid State Commun.* **25** 93
[33] Hermanson J 1977 *Solid State Commun.* **22** 9
[34] Lapeyre G J and Anderson J 1979 *Surf. Sci.* **89** 304
[35] Borstel G, Neumann M and Wohlecke M 1981 *Phys. Rev.* B **23** 3121
[36] Zangwill A 1987 *Giant Resonance in Atoms, Molecules and Solids* ed. J P Connerade *et al* (New York: Plenum) p 321
[37] Rau C and Robert M 1987 *Phys. Rev. Lett.* **58** 2714
Rau C and Eicher S *Nuclear Methods in Materials Research* ed. K Bethge *et al* (Braunschweig: Vieweg) p 354
[38] Rau C and Eichner S 1986 *Phys. Rev.* B **34** 6347
[39] Weller D, Alvarado S F, Gudat W, Schroder K and Campagna M 1984 *Phys. Rev. Lett.* **54** 1555
[40] Jepson O, Madsen J and Anderson O K 1982 *Phys. Rev.* B **26** 2790
[41] Eberhardt W and Plummer W W 1980 *Phys. Rev.* B **21** 3245
[42] Carbone C and Kisker E 1987 *Phys. Rev.* B **36** 1280
[43] Varma S, Kime Y J, Dowben P A, Onellion M and Erskine J L 1986 *Phys. Lett.* **116A** 66
[44] Onellion M, Dowen P A and Erskine J L 1988 *Phys. Lett.* **130A** 171
[45] Dowben P A, Sakisaka Y and Rhodin T N 1985 *J. Vac. Sci. Technol.* A **3** 1855
[46] Davis L C 1986 *J. Appl. Phys.* **59** R25
[47] Schutz G, Knulle M, Wienke R, Wilhelm W, Wagner W, Kienle P and Frahm R 1988 *Z. Phys.* B **73** 67
[48] Dowben P A, Varma S, Kime Y J, Onellion M and Erskine J L 1987 *Phys. Rev.* B **36** 2519
[49] Mertzbacher E 1970 *Quantum Mechanics* (New York: Wiley)
[50] Orchard A F and Thornton G 1978 *J. Electron Spectrosc. Relat. Phenom.* **13** 27
[51] Beatham N, Cox P A, Orchard A F and Grant I P 1979 *Chem. Phys. Lett.* **63** 69
[52] Shirley D A 1978 *Photoemission in Solids I* ed. M Cardona and L Ley *Topics in Applied Physics* vol 26 (New York: Springer) p 165
[53] McFeely F R, Kowalczyk S P, Ley L and Shirley D A 1974 *Phys. Lett.* **49A** 301

[54] Gupta R P and Sen S K 1974 *Phys. Rev.* B **10** 71
[55] Fadley C S, Shirley D A, Freeman A J, Bagus P S and Mallow J V 1969 *Phys. Rev. Lett.* **23** 1397
[56] Bagus P S, Freeman A J and Sasaki F 1973 *Phys. Rev. Lett.* **30** 850
[57] Freeman A J and Watson R E 1965 *Magnetism* vol 2a ed. G Rado and H Suhl (New York: Academic) p 167
[58] Centre for X-ray Optics 1986 *X-ray Data Booklet* (Lawrence Berkeley Laboratories)
[59] Sakisaka Y, Dowben P A and Rhodin T N 1984 *Solid State Commun.* **49** 563